

# Design Considerations For Parabolic-Cylindrical Solar Collectors

George W. Treadwell

Prepared by Sandia Laboratories, Albuquerque, New Mexico 87115  
and Livermore, California 94550 for the United States Energy Research  
and Development Administration under Contract AT(29-1)-789

Printed July 1976

***When printing a copy of any digitized SAND Report, you are required to update the markings to current standards.***



Sandia Laboratories  
energy report



Issued by Sandia Laboratories, operated for the United States Energy Research and Development Administration by Sandia Corporation.

---

#### **NOTICE**

This report was prepared as an account of work sponsored by the United States Government. Neither the United States nor the United States Energy Research and Development Administration, nor any of their employees, nor any of their contractors, subcontractors, or their employees, makes any warranty, express or implied, or assumes any legal liability or responsibility for the accuracy, completeness or usefulness of any information, apparatus, product or process disclosed, or represents that its use would not infringe privately owned rights.

SAND76-0082  
Unlimited Release  
Printed July 1976

Distribution  
Category UC-62

DESIGN CONSIDERATIONS FOR PARABOLIC-CYLINDRICAL SOLAR COLLECTORS

George W. Treadwell  
Solar Energy Project Division 5712  
Sandia Laboratories  
Albuquerque, NM 87115

ABSTRACT

This report presents in some detail the various significant factors which influence the design of parabolic-cylindrical solar collectors.

Printed in the United States of America

Available from  
National Technical Information Service  
U. S. Department of Commerce  
5285 Port Royal Road  
Springfield, Virginia 22161  
Price: Printed Copy \$5.00 ; Microfiche \$2.25

## ACKNOWLEDGMENT

The foundation for much of the work described in this report comes from the efforts of a number of technical research personnel within Sandia Laboratories. An exhaustive listing is not practical, but appreciation for their contributions is extended to the following:

Coating Development - D. M. Mattox, 5834, R. R. Sowell, 5834

Optical and Thermophysical Properties - R. B. Pettit, 5842

Reflector Characterization - B. L. Butler, 5844

Code Development - M. W. Edenburn, 5719; W. H. McCulloch, 5711  
F. Biggs, 5231

## CONTENTS

	<u>Page</u>
Summary	7
Introduction	8
Considerations	9
Solar Coating	9
Sizing of Glass Annulus	13
Insulating or Silvering of Glass	16
Reflection and Transmittance	17
Receiver Tube Sizing	21
Collector Sizing	29
Influence of Asymmetric Heating	30
Other Design Considerations	30
Miscellaneous Considerations	33
APPENDIX A - CALCULATION OF RIM ANGLE FOR MINIMUM AVERAGE DISTANCE FROM FOCUS TO PARABOLA	35
Bibliography	37

## TABLES

<u>Table</u>	<u>Page</u>
I      Average Collector Efficiency Percentage at 316°C (600°F)	16
II     Phase IVB Collector Sizing Considerations	26
III    Collector Efficiency (%) and Arc Length Changes (%) Compared to 1.57 Radians (90°) Rim Angle	27
IV     Figure of Merit vs Collector Rim Angle	28

## FIGURES

<u>Figure</u>	<u>Page</u>
1      Parabolic-Cylindrical Solar Collector	8
2      Reflector With Receiver Tube Suspended at Focal Line	10
3      Reflector With Glass-Jacketed Receiver Tube Suspended at Focal Line	10
4      Input Temperature vs Percent Efficiency for 25.4 mm OD Receiver With 57.1 mm OD Glass Jacket at No Vacuum	11
5      Input Temperature vs Percent Efficiency for 25.4 mm OD Receiver With 57.1 mm OD Glass Jacket at 0.2 mm Hg Pressure	11
6      Solar Collector Test Results	12
7      Total Hemispherical Emittance of Receiver vs Collector Efficiency	12

CONTENTS (cont)

FIGURES

<u>Figure</u>		<u>Page</u>
8	Harshaw Black Chrome on Electroplated Sulfamate Nickel (4 Minute Treatment Time)	13
9	Harshaw Black Chrome (4 Minute Treatment Time)	14
10	Steel Receiver With Glass Jacket	15
11	Results Obtained From Equation (1)	15
12	Receiver Cross Section	17
13	Collector Power Losses	18
14	Collector Power Losses	18
15	Probable Collector Efficiency Range	19
16	Solar Spectrum Reflectance vs Aperture For Various Reflector Materials	20
17	Collector Efficiency vs Non Non Normal Sun Position (Assuming Attenuation at Solar Noon Applied to All Sun Angles)	20
18	Receiver Tube Assembly Cross Section	21
19	Various Rim Angles for Common Aperture	22
20	Energy Distribution vs Collector Efficiency	23
21	Apparatus for Characterizing Slope Errors of Parabolic Reflector Surfaces	24
22	Scans Resulting From Use of Apparatus Shown in Figure 21	24
23	Collector Efficiency vs Receiver Tube Outer Diameter	26
24	Influence of Off-Center Receiver Tube Mounting	28
25	Energy Input Influence on Receiver Sizing	29
26	Predicted Maximum Therminol 66 <sup>Ⓟ</sup> Film Temperatures	31
27	Influence of Plug on Predicted Maximum Therminol 66 <sup>Ⓟ</sup> Film Temperatures (Phase IVA Northwest Quadrant)	31
28	Receiver Tube and Support Assembly	32
29	Alternate Receiver Tube Assembly Design	33

## DESIGN CONSIDERATIONS FOR PARABOLIC-CYLINDRICAL SOLAR COLLECTORS

### Summary

The solar collector is an important component in the solar powered system presently being designed and installed at Sandia Laboratories. This report describes some of the key considerations which have an influence upon collector design.

The relative importance of the solar coating absorptance and total hemispherical emittance for linear-focusing collectors is described. A high absorptance has a much more important effect on collector efficiency than does a low emittance. The evacuation of a glass-jacketed receiver design achieves approximately a 5% efficiency improvement, and the design is shown to be sized with the least thermal loss strategy when the annulus gap between the steel receiver and glass is approximately 10 mm (0.4 in.). The tradeoffs between an insulated or silvered glass jacket and total hemispherical emittance are also shown. When the emittance is greater than 0.5 an insulated glass jacket is desirable. Silvering the glass is of dubious benefit under any conditions because of processing and durability considerations.

The present state of the art in reflecting materials is used in energy balance calculations, and the calculated results are compared to test results to illustrate plausible improvements in collector efficiency. Durable specular reflective surfaces with reflectivity between 0.90 and 0.95 are presently being fabricated in laboratory sizes. It is reasonable to expect that efficiencies of 70% at 315°C and solar noon can be achieved in the near future. The interrelationships between reflector rim angle and receiver size are shown to result in rim angle selections which maximize energy collection for minimal costs. Although a 2.09 radians (120°) rim angle has the minimum average parabola-to-focus distance, a reasonable rim angle is shown to be 1.57 radians (90°) because of minimal collector efficiency improvements with accompanying increased construction costs for 2.09 radians (120°). The characterization of parabolic reflector shapes and reflector materials are part of this selection process. Mirror slope standard deviations of less than 9 milliradians (0.5°) are achievable. The relationship between optical congruency and thermal non-congruency in establishing optimal collector sizing is also demonstrated. A 2-metre wide aperture is shown to be reasonable for systems which allow 1% of the collected energy to be used for pumping.

The importance of asymmetric heating on the receiver design is described in some detail as is the importance of flow control when organic heat transfer liquids are used. With a 25 mm OD receiver, a 2-metre aperture width, and a 1.57 radian rim angle, flow rates of greater than 0.00019 m<sup>3</sup>/sec (3gpm) are required in order to prevent local overheating and eventual destruction of the organic liquid. A lower flow rate could be achieved by incorporating internal liquid turbulence generators.

A limited discussion of collector orientations and off-axis receivers is included. Collector fields oriented north-south collector more energy than do east-west oriented fields but are less economical in land utilization because of nonshadowing spacings, in pipeline costs, in structural costs, and in thermal losses.

### Introduction

Sandia Laboratories has been funded by the Energy Research and Development Administration to analyze, design, and build a solar total energy experimental system to provide the energy needs for a 1100 square-metre building.

A significant contributor to a successful solar-powered system is the design of the solar collector. The design of the collector must be such that energy capture is high, thermal losses are low, and cost/effectiveness ratio is as small as practicable. This report addresses the design of parabolic-cylindrical solar collectors (Figure 1) using Therminol 66<sup>®</sup> heat transfer liquid in uniflow receiver tubes and examines in some detail those aspects most important to high collector efficiency; it briefly examines cost aspects since production quantities have such a large influence upon unit costs.

One of the purposes of this report is to portray the relationships between the sizes and shapes of these collectors. An understanding of these relationships will allow comparisons and analyses to be drawn for other focusing collector designs. It should be noted that this report examines, only cursorily, matters such as collector orientation, equatorial mount tracking, and collector field layouts. These matters have been more properly treated in detail in other reports.

Some of the work described in this report is extracted from the sources listed in the bibliography particularly with respect to the use of the listed computer codes, spectrum definitions, material characteristics, and heat transfer phenomena. Other opinions and results are based upon nearly three years of experience in testing, measuring, construction, and analyses at Sandia Laboratories. This report is not intended to be a parametric sensitivity analysis, but it does examine what is believed to be the more important facets of design in a 315°C (600°F) maximum operating temperature system. Reference to the bibliography will permit a more thorough examination of some of these aspects.

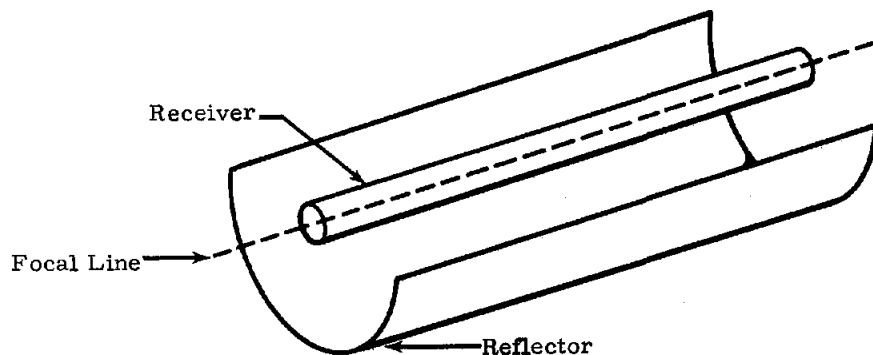


Figure 1. Parabolic-Cylindrical Solar Collector

## Considerations

### Solar Coating

Several authors have attempted to describe the importance of a coatings' high average solar energy absorptance ( $\alpha_S$ ) and total hemispherical emittance ( $\epsilon_{TH}$ ) ratio ( $\alpha_S/\epsilon_{TH}$ ). In reality, the ratio is not very important and this will be illustrated by reference to test results and to analysis. A Pyromark<sup>®</sup> - painted ( $\alpha_S = 0.98$ ,  $\epsilon_{TH(300^\circ C)} = 1.0$ ) receiver tube suspended at the focal line of a 1.57 radians (90°) rim angle Alzak<sup>®</sup> reflector (Figure 2) oriented normal to the sun, was unable to capture sufficient reflected energy to compensate for thermal losses at 315°C (600°F) and operated at a negative efficiency (defined as: energy into liquid in receiver/energy into aperture). The addition of a glass jacket (Figure 3) allowed a positive efficiency to be obtained (Figure 4). The use of a modest vacuum in the annulus improved the efficiency approximately 5% (Figure 5). The range of analytical-model predicted results compared with some test results are shown in Figure 6. Since the Alzak has a specular reflectance within the portrayed range, there is reasonable agreement between predictions and test results

Since the test results and analytical model have reasonable agreement, an analytical model was used to calculate the data appearing on Figure 7 and to portray the influence of  $\alpha_S$  and  $\epsilon_{TH}$ . From these data, a clear relationship between solar absorptance and total hemispherical emittance can be seen. The higher the  $\alpha_S$ , the higher the collector efficiency; the lower the  $\epsilon_{TH}$ , the higher the collector efficiency, but the improvement is not so pronounced. The collector efficiency with

$$\alpha_S = 0.85 \text{ and } \epsilon_{TH} = 0.05 \left( \frac{\alpha_S}{\epsilon_{TH}} = 17 \right)$$

is 50%; the collector efficiency with

$$\alpha_S = 0.95 \text{ and } \epsilon_{TH} = 0.3 \left( \frac{\alpha_S}{\epsilon_{TH}} = 3.17 \right)$$

is 51%. It is obvious from these data that a high absorptance is far more important than a low emittance, and the ratio of  $\alpha_S/\epsilon_{TH}$  not so important. In other words, it is far more effective to initially capture the sun's energy and attempt to decrease those thermal losses controlled by the emittance through proper design.

Coating development work at Sandia and NASA/Lewis has demonstrated that a thin (0.15-0.20  $\mu\text{m}$ ) black chrome ( $\text{Cr}_2\text{O}_3$ ) layer electrodeposited over dull nickel can achieve  $\alpha_S \geq 0.95$  and  $\epsilon_{TH} \leq 0.25$  and not degrade rapidly at operating temperatures of at least 315°C whether exposed to air, moisture, and/or ultraviolet energy. The coating's total hemispherical emittance determined by calorimetric techniques is displayed as a function of temperature in Figure 8. In general, the emittance is directly proportional to the electrodeposition time and

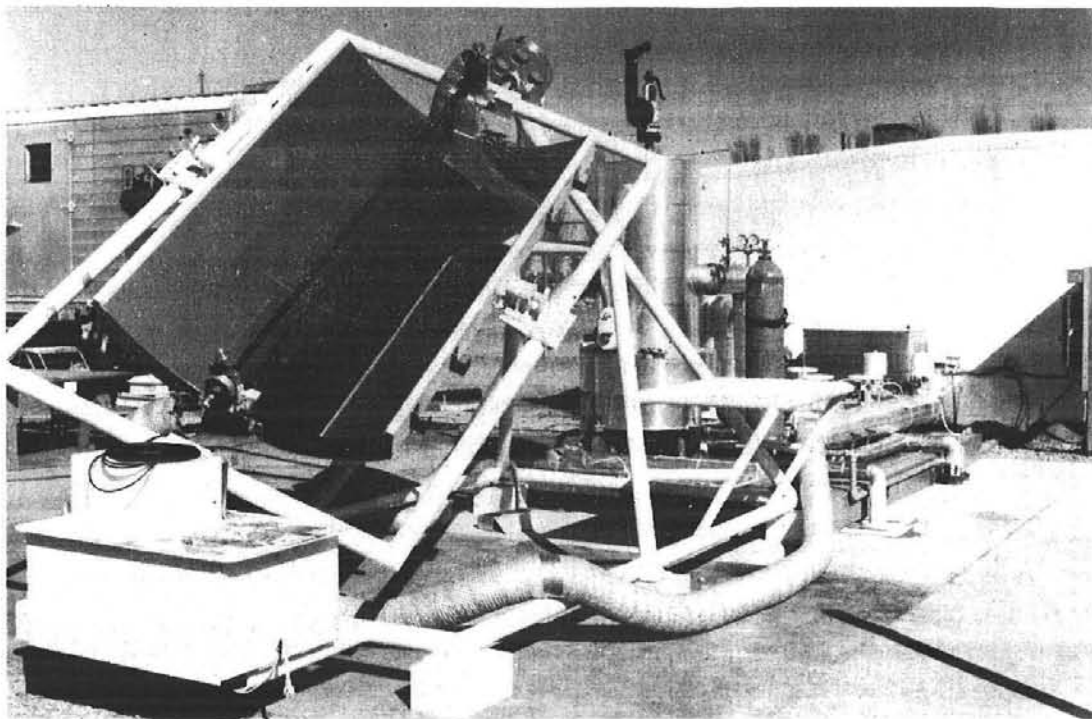


Figure 2. Reflector With Receiver Tube Suspended at Focal Line

Receiver Tube  
1.00 in. OD 25.4 mm  
Pyromark  
2.25 OD Glass 57.1 mm  
0.5 Annulus Evacuated 12.7 mm  
To 0.1 mm Hg

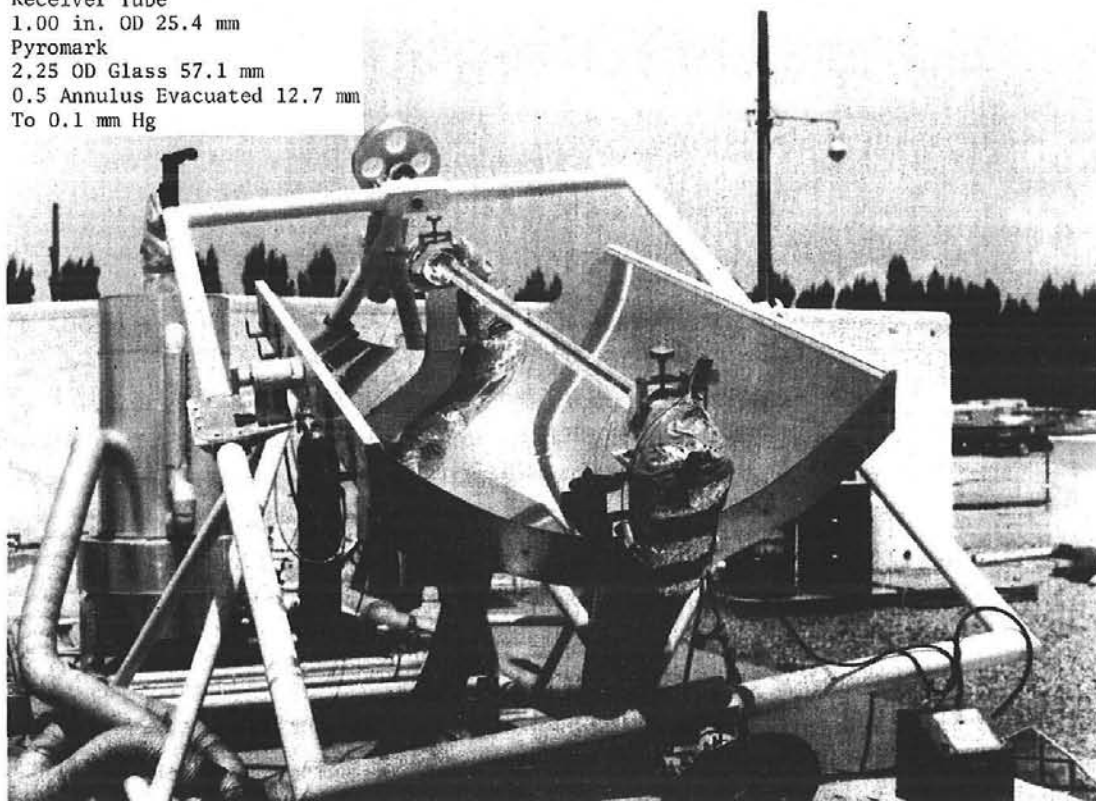


Figure 3. Reflector With Glass-Jacketed Receiver Tube Suspended at Focal Line

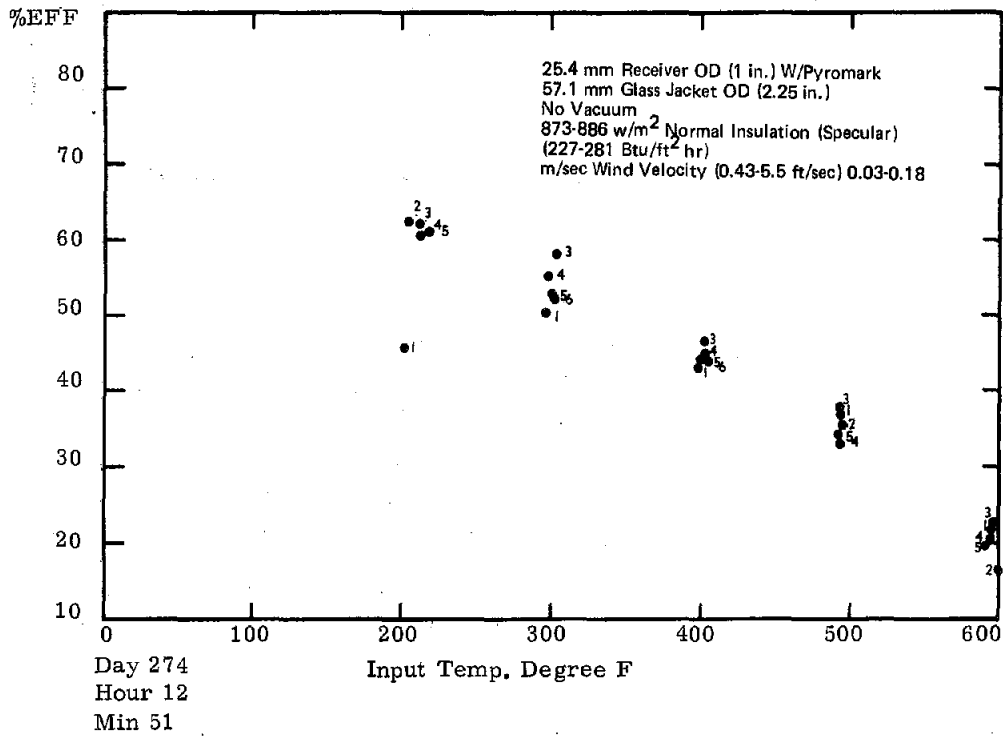


Figure 4. Input Temperature vs Percent Efficiency for 25.4 mm OD Receiver With 57.1 mm OD Glass Jacket at No Vacuum

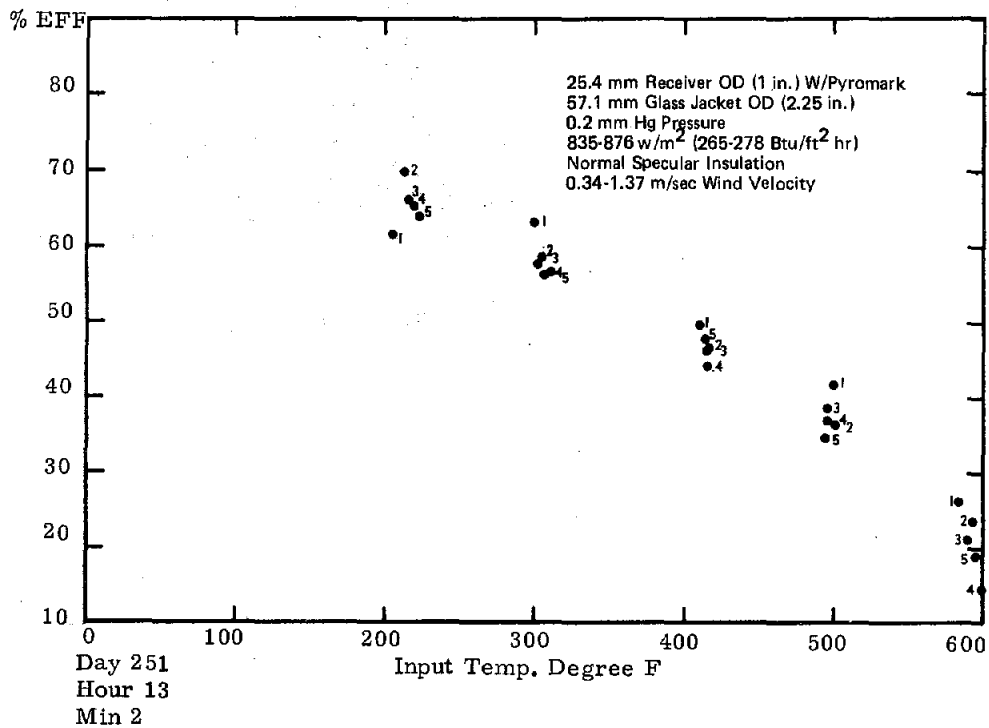


Figure 5. Input Temperature vs Percent Efficiency for 25.4 mm OD Receiver With 57.1 mm OD Glass Jacket at 0.2 mm Hg Pressure

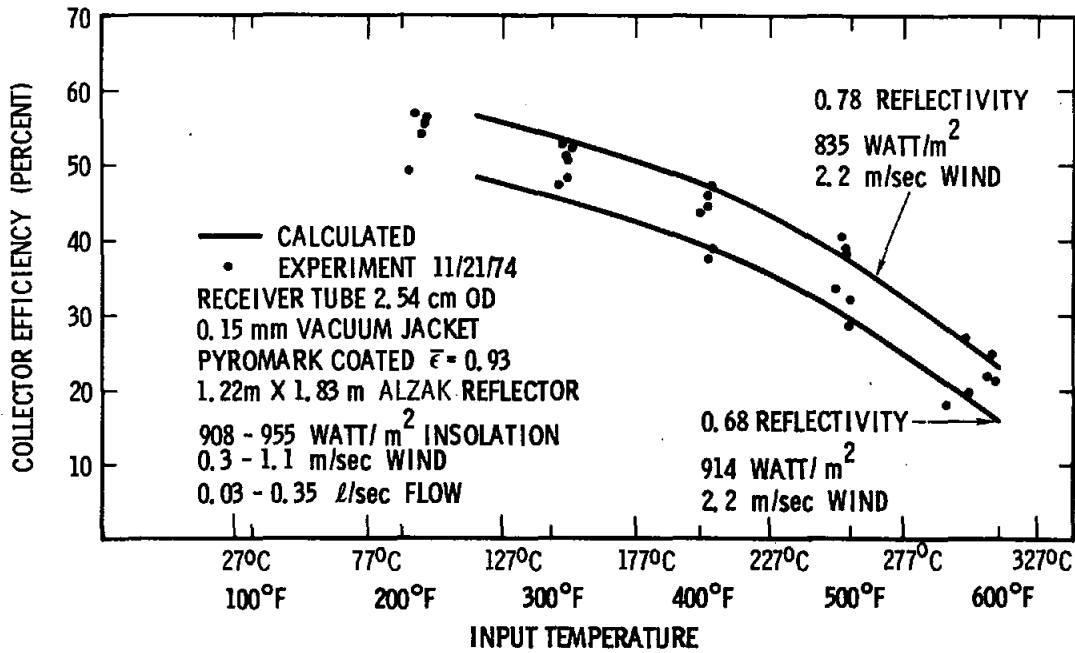


Figure 6. Solar Collector Test Results

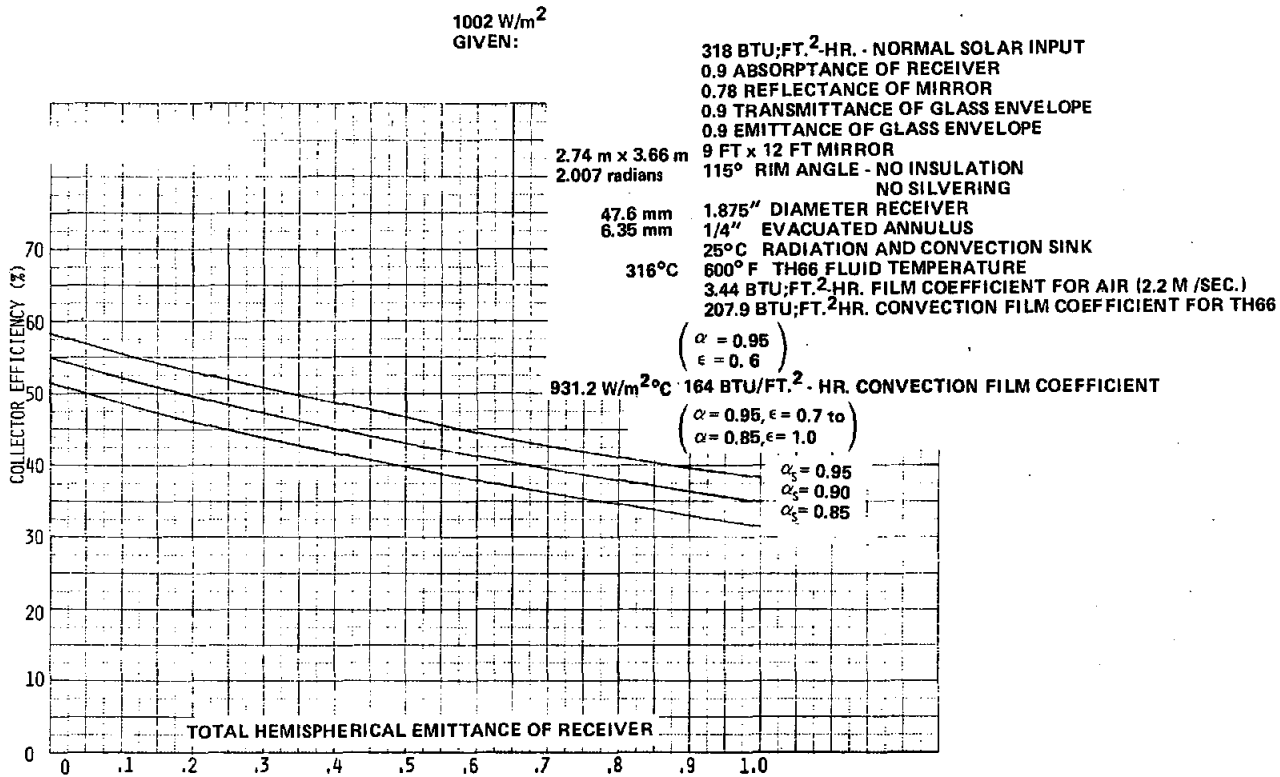


Figure 7. Total Hemispherical Emissance of Receiver vs. Collector Efficiency

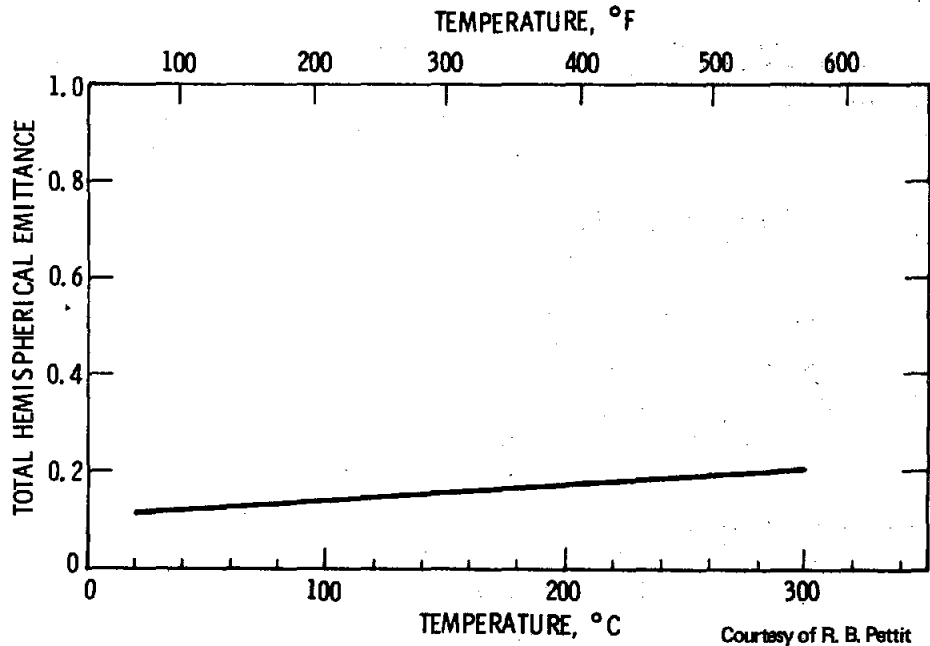


Figure 8. Harshaw Black Chrome on Electroplated Sulfamate Nickel (4 Minute Treatment Time)

current levels in the bath. On the other hand, the absorptance increases to a plateau maximum with increases in plating times. The plating time for black chrome is established to achieve  $\alpha_s \geq 0.95$  and, with that timing and current density, achieves  $\epsilon_{TH}(300^\circ\text{C}) \leq 0.25$ . Solar absorptance of a solar coating decreases with increasing angles of incidence, and black chrome is no exception. Figure 9 shows the changes in  $\alpha_s$  as the angle increases. This phenomenon must be factored into the sizing considerations for solar receiver tubes. This will be described later.

Other coatings, particularly vacuum-deposited multiple interference coatings, can achieve the solar characteristics of black chrome but not necessarily at as low a production price. As of April 1975, a quoted price for black chrome over nickel was  $\$13.89/\text{m}^2$  ( $\$1.29/\text{ft}^2$ ) in 23 226  $\text{m}^2$  (250,000  $\text{ft}^2$ ) quantities. Projections from available data suggest production prices as low as  $\$.50/\text{ft}^2$  are ultimately achievable.

#### Sizing of Glass Annulus

In the previous section, the need for a transparent glass jacket to significantly reduce thermal convection losses from the surface of the receiver tube was demonstrated. The annulus size which will minimize losses from the system can be determined. Since the transmission of solar energy through glass is a function of thickness, the glass should be only thick enough to withstand structural loading and reasonable hail threats.

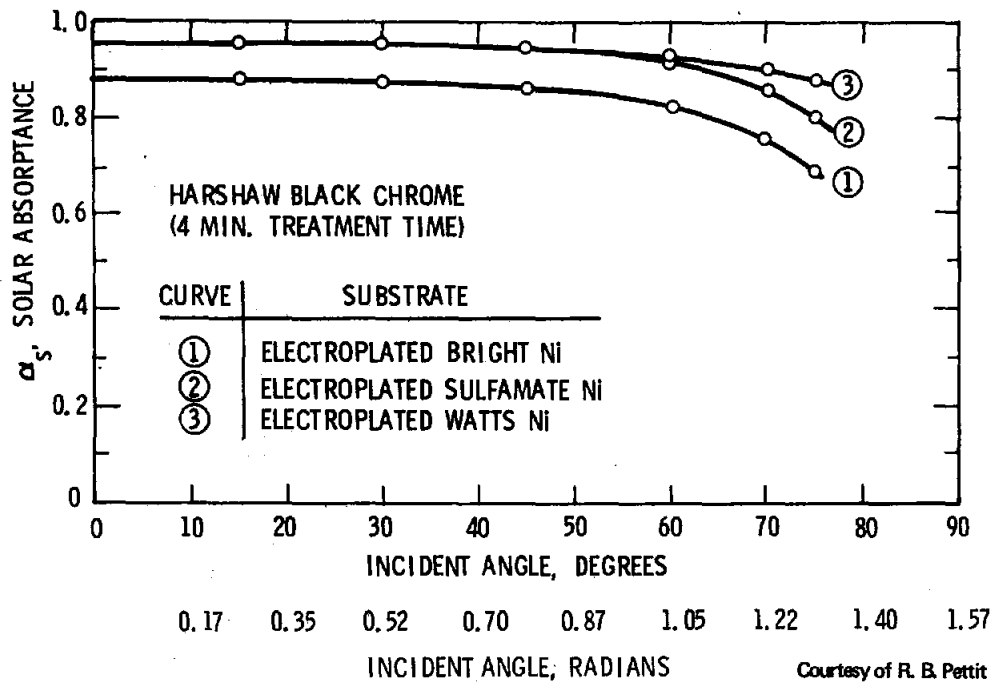


Figure 9. Harshaw Black Chrome (4 Minute Treatment Time)

A simplified technique used for annulus sizing is somewhat analogous to the determination of critical insulation thickness for small-diameter circular tubes. An energy balance for a given operating temperature can be constructed as follows: Radiation loss from the coated receiver tube + air conduction and convection loss from the coated receiver tube = convection loss to environment from glass tube + radiation loss to environment from the glass tube. The algebraic formulation of the configuration shown in Figure 10 is as follows:

$$\frac{\sigma A_1 (T_1^4 - T_2^4)}{\epsilon_1 + \frac{A_1}{A_2} \left( \frac{1}{\epsilon_2} - 1 \right)} + \frac{2\pi k_e L (T_1 - T_2)}{\ln \left( \frac{r_2}{r_1} \right)} = h_2 A_2 (T_2 - T_a) + \sigma \epsilon_2 F_{2a} A_2 (T_2^4 - T_a^4) \quad (1)$$

where

h = heat transfer coefficient	L = length
σ = Stefan-Boltzmann constant	k <sub>e</sub> = effective thermal conductivity
ε = emittance	F = radiation shape factor
A = area	

In the case of a vacuum in the annulus, the second expression on the left is not considered since  $k_e \rightarrow 0$ .

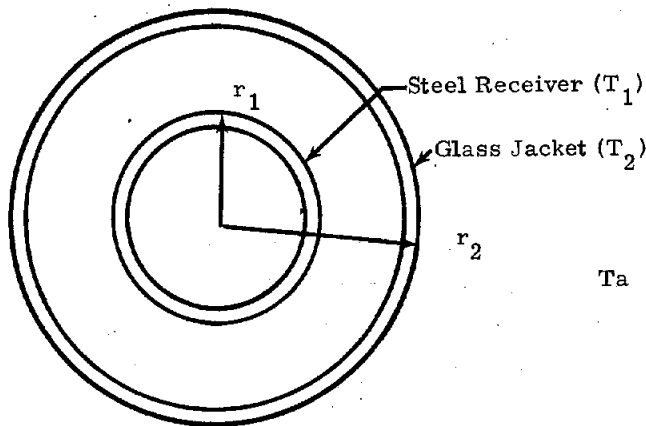


Figure 10. Steel Receiver With Glass Jacket

Some of the results from this equation are shown in Figure 11. The optimum annulus gap is established through a review of these data. If operation with a vacuum could be guaranteed, it would be desirable to establish the annulus gap as its minimum possible size to minimize the unit length thermal losses, as per Curve B. However, if the vacuum is lost, the losses would be expressed by Curve D for that particular gap. From this, it is evident that the gap should be selected to be at the minimum of Curve D since Curve B (vacuum) losses for that larger gap (~11mm) are slightly greater but vacuum failure will result in the minimum system thermal losses. At an operating temperature of 204°C, the conduction-convection losses shown by Curve A still are minimum at a gap of approximately 11 mm (0.44 in.). A doubling of the convection film coefficient ( $h_2$ ), and a halving of the receiver diameter still results in an optimum gap of between 9.5 and 11 mm.

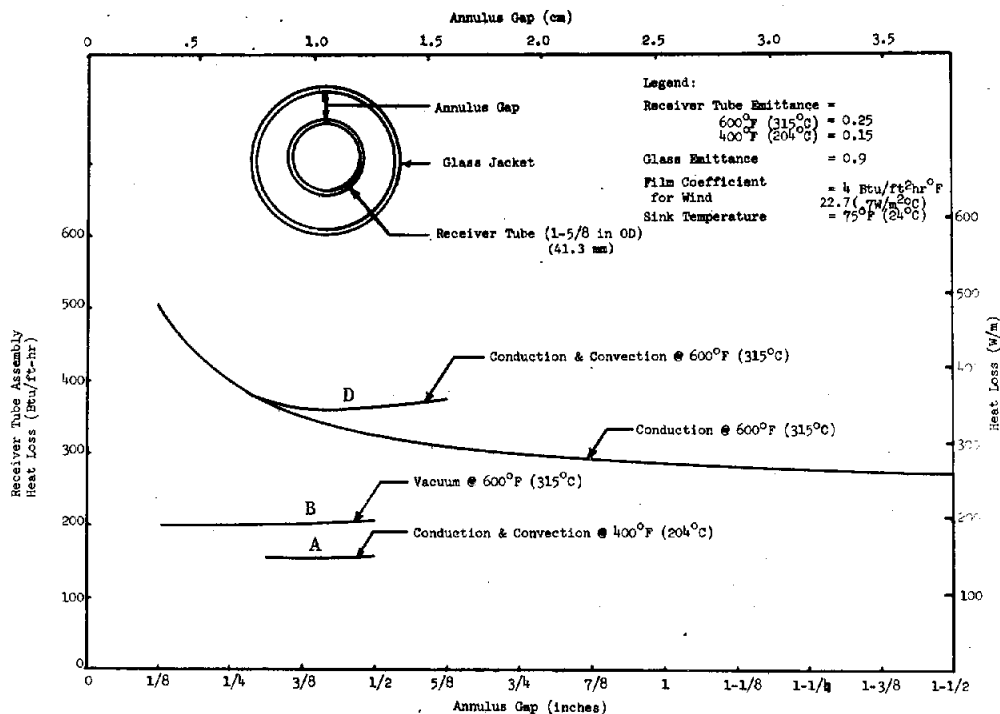


Figure 11. Results Obtained From Equation (1)

Curve B has only a slight positive slope and Curve D has a broad trough so with consideration of production tolerances and gravity sag, an annulus size of between 9.5 mm and 12.7 mm would be adequate for the parameters used in the calculations.

### Insulating or Silvering of Glass

Upon initial consideration, it might seem appropriate to either silver or insulate an arc of glass opposite the reflector (Figure 12) to decrease thermal losses. Actual test results, reported in Table I, refute that supposition as a general conclusion. Only in the case of high total hemispherical emittance ( $> 0.5$ ) is there an improvement in collector efficiency. With a 1.57 radians arc of insulation to preclude additional reflector shadowing, a high-emittance receiver increased in efficiency; an insulated low-emittance receiver decreased in efficiency for the same test configuration. With a high-emittance coating, the insulating strip more than compensates in thermal savings for the loss of the direct sun on the receiver tube. With a low-emittance coating, the thermal losses are already so low that decreasing them still further cannot compensate for the occlusion of the direct sun.

TABLE I  
Average Collector Efficiency Percentage at 316°C (600°F)

Receiver Tube Coating	No Vacuum	Vacuum	Vacuum w/Insulator	Vacuum w/Plug	No Vacuum w/Plug	Remarks
Pyromark (Tempil) ( $\alpha = 0.98, \epsilon = 1.0$ )	16.2	18.32	23.9	X	X	Average of 10 days' data for vacuum no vacuum. Average of 4 days' data for vacuum w/insulator.
Intermediate Black Chrome on Bright Nickel ( $\alpha = 0.88, \epsilon = 0.24$ )	32.1	34.6				Average of 8 days' data.
AMA (Honeywell) ( $\alpha = 0.97, \epsilon = 0.38$ )	39.0	43.1	42.2			Average of 5 days' data; vacuum w/insulator, 1 day average
Black Chrome on Sulfamate Nickel ( $\alpha = 0.97, \epsilon = 0.28$ )	41.6	46.2	43.1		X	Average of 9 days' data for vacuum/no vacuum. Average for 6 days' data for vacuum w/insulator.

- NOTES: 1. Volume flow rate approximately 5.7 l/min (1.5 gpm) ( $Re > 12,000$ ).  
 2. Test temperature varied between 302°C (575°F) and 311°C (591°F).  
 3. Collector Efficiency Percentage =

$$\frac{\dot{m} C_p (T_{OUT} - T_{IN})}{(\text{Aperature Area}) (\text{Direct Insolation})}$$

4. Direct Insolation Range: 861-990 W/m<sup>2</sup> (273-314 Btu/ft<sup>2</sup>/hr).  
 5. Wind Velocity Range: 0.24-3.46 m/sec (0.73-11.4 ft/sec).  
 6. Internal cylindrical plug of 1.59 cm (5/8") dia.  
 7. X = To be tested.  
 8. Alzak Reflector ( $\rho \approx 0.7$ ).

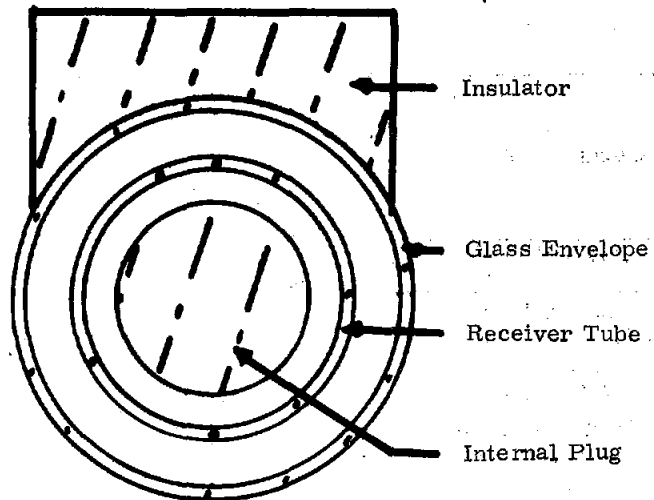


Figure 12. Receiver Cross Section

This analogy would hold for the silver coating also. In addition, the silver should be deposited on the inner surface of the glass which means a diffuse surface would face the receiver and not necessarily reflect the infrared energy due to radiation back to the receiver. Further, as time passes, the silver would change in infrared reflectance as imperfect vacuums allow oxygen to attack the surface.

With these considerations, neither insulation nor silvering are recommended for the low-emittance coatings contemplated for use.

#### Reflection and Transmittance

Examination of the collector energy losses for normal incidence, (Figure 13) indicates that significant improvements in collector efficiency can be made through improvements over the present technology for parabolic mirror reflectance and glass jacket transmission. Figure 14 illustrates the influence of a ten percentage point change in mirror reflectance. The coating losses shown are given by  $(1 - \alpha_S)$ , and can be improved only slightly by increasing the coating absorptance. The thermal losses, convection and radiation, are substantially only a function of operating temperature as long as the receiver internal design effectively permits energy to be delivered into the energy collecting liquid. Should the desired improvements be made in the optics losses (coating absorptance, mirror reflectance, and glass transmission), Figure 15 illustrates the collector efficiency improvements which can be realized. For every percentage point increase in either reflectance or transmission, the collector efficiency increases nearly a percentage point.

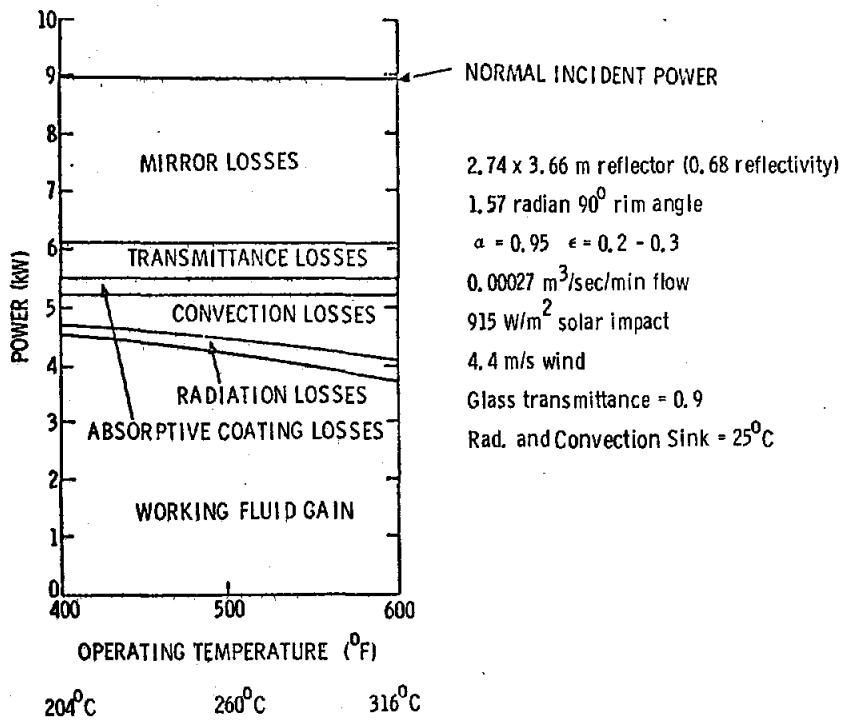


Figure 13. Collector Power Losses

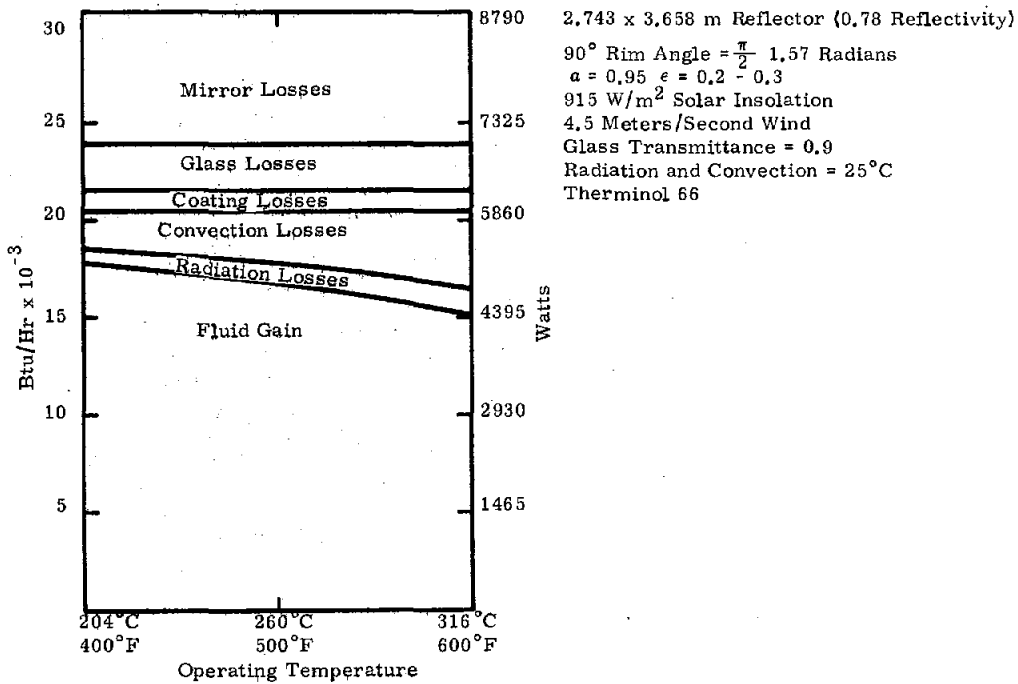


Figure 14. Collector Power Losses

PROBABLE COLLECTOR EFFICIENCY RANGE

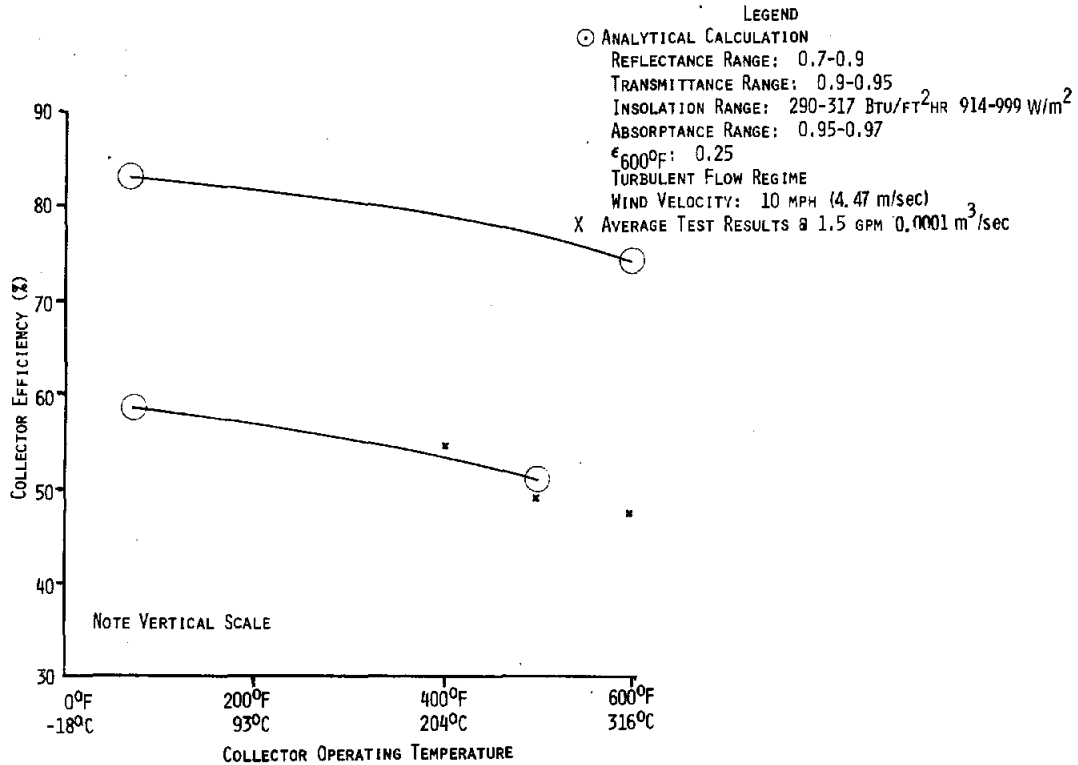


Figure 15. Probable Collector Efficiency Range

Although durable reflectors with a specular reflectance,  $\rho$ , of 0.95 are not presently available in large size, laboratory-sized specimens are available and development efforts are underway to increase size. An important characteristic of the reflectance is its specularity, and this is measured as a function of angular aperture. Figure 16 illustrates the solar reflectance versus aperture of several reflector materials of the present and near future. The aperture angle occluded by a receiver tube dictates the specular reflectance characteristics that are appropriate for use in analytical calculations. It can be seen that Alzak<sup>Ⓢ</sup> has directional characteristics that must be taken into consideration in design.

The influence of energy reflections off the glass jacket if the sun is non-normal, as is the preponderant situation for east-west oriented parabolas, is shown in Figure 17. The maximum attainable efficiency curve is also displayed to illustrate the magnitude of improvement that could be obtained with no reflectance loss off the glass and coating. This chart does not include end loss effects whereby energy reflected off the end of the reflector is lost in space. The application of an inexpensive antireflection coating on, say, soda-lime glass could increase the transmission,  $\tau$ , from 0.90 to 0.95. Present efforts indicate a fluoroboric acid vapor attack of soda-lime glass can achieve this improvement. If an antireflection coating is not applied, significant decreases in daily energy collection can be expected for east-west oriented collectors in addition to the cosine and end losses.

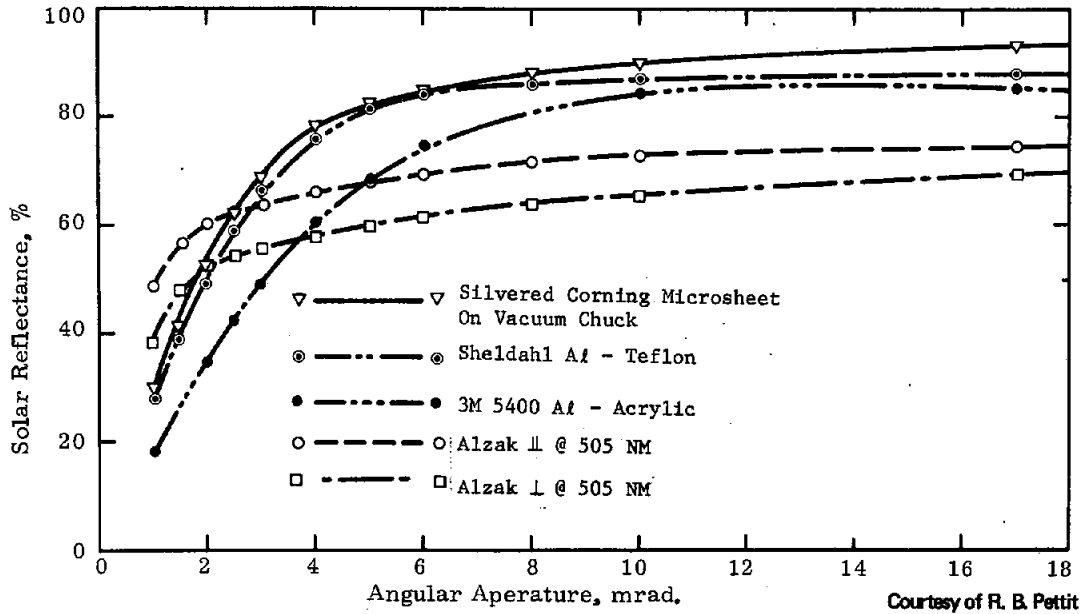


Figure 16. Solar Spectrum Reflectance vs Aperture For Various Reflector Materials

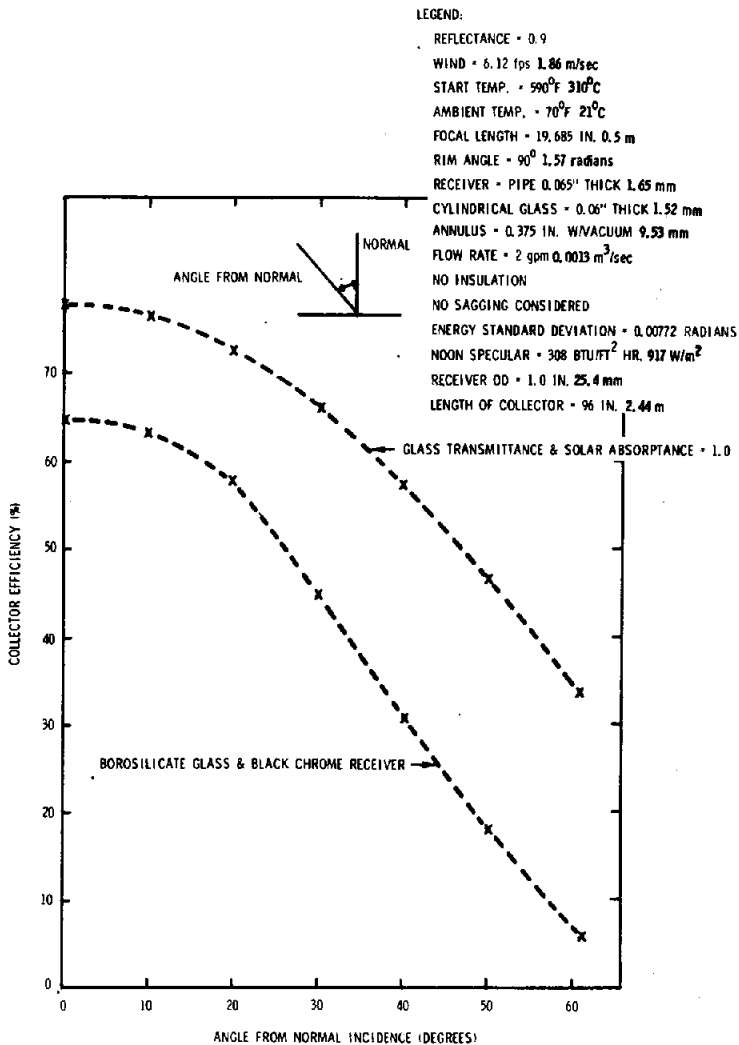
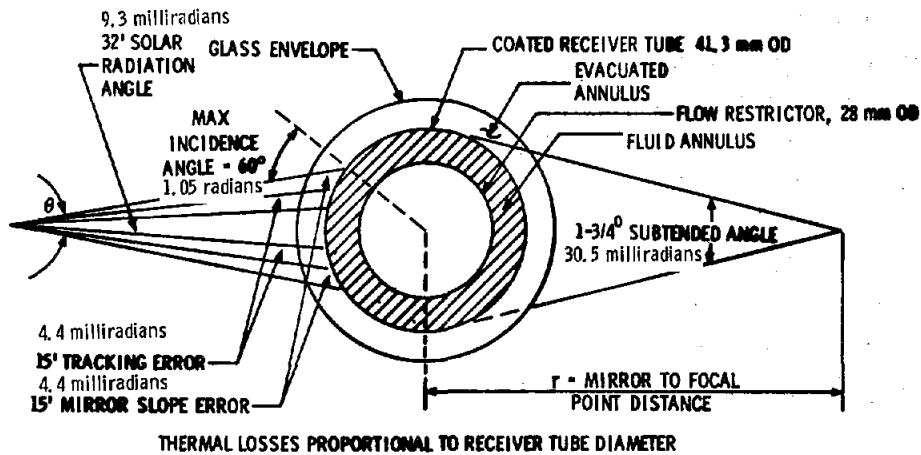


Figure 17. Collector Efficiency vs Non-Normal Sun Position (Assuming Attenuation at Solar Noon Applied to All Sun Angles)

Receiver Tube Sizing

In an initial approximation for the sizing of the receiver tube diameter, the assumption can be made that it is appropriate to attempt to capture all of the energy reflected from the parabola. The receiver tube size would then be dependent upon the sun's angular width (0.009 radians of arc), the magnitude of the tracking error, the mirror slope error (i.e., the angular departure from a tangent to a theoretical parabola), the irregularity of the reflective surface, and the angular absorptance characteristics of the solar coating. Figure 18 sums these influencing factors in a conservative arithmetic manner since the potential magnitude of tracking and slope errors is not completely known. The 1.05 radians maximum incidence angle conservatively compensates for photon reflection off the solar coating. From this figure, since the sizing is in terms of angular aperture, it can be seen that the receiver diameter is proportional to the distance from the reflector.

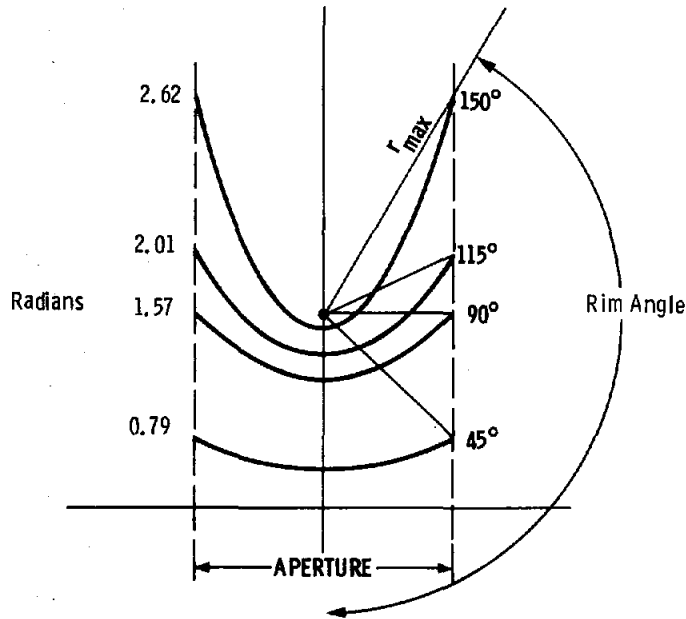
It is also apparent from Equation (1) that thermal losses are directly proportional to the receiver diameter, so the obvious goal would be to select a parabolic rim angle which would result in the smallest maximum distance from parabola to focus. A review of several rim angles for a common aperture (Figure 19) results in the selection, by calculation from Figure 18 and by inspection, of a rim angle of 1.57 radians. This angle will minimize the maximum reflector-to-focus distance and therefore require the smallest receiver diameter. When the aperture width is established, the receiver diameter can then be calculated. For example, with a 2-metre aperture the calculated receiver diameter is 30.9 mm.



$$\text{RECEIVER TUBE DIAMETER} = \frac{2r \sin \theta/2}{\sin 60^\circ \sin (\text{RIM ANGLE})}$$

Figure 18. Receiver Tube Assembly Cross Section

### RIM ANGLE SELECTION



FOR COMMON FOCUS AND FIXED APERTURE:  
 $r_{max}$  IS MINIMUM @ RIM ANGLE OF 90°

Figure 19. Various Rim Angles for Common Aperture

When one considers the implication of the central limit theorem, i. e., the distribution of the sum of several random variables can be closely approximated by a normal distribution, it is possible that receiver tubes sized in accordance with the preceding conservative rationale may not be of optimum size. While assumptions must still be made regarding the tracking and slope error potential and mirror non-specularity, trade-offs can be made between the amount of solar energy which can be allowed to miss a smaller receiver tube and the compensating savings in thermal losses through diameter reduction. A portrayal of such trade-offs for assumed errors and normal solar incidence is shown on Figure 20. For an energy distribution standard deviation\* ranging from minimum (the sun's quarter-width) to 12 milliradians, it can be observed that the optimum receiver diameter is a function of the energy distribution. The use of the apex connecting line permits the determination of an optimum diameter once the energy distribution is known. Since thermal losses are a function of the receiver surface area, it also can be observed that for a given energy distribution other shapes of receivers to decrease surface area, (i.e., triangular or flattened circles) would have a modest influence on collector efficiency because of the broad shapes of the curves. For example, with an energy distribution of 7.72 milliradians, small efficiency differences are observed within a receiver diameter range of between 22.2 mm and 30.9 mm. As the energy distribution arc becomes smaller, the receiver diameter becomes of greater importance.

\*The statistical blending of the sun's width, tracking errors, slope errors, and mirror diffuseness:

$$\sigma_{Total} = \sqrt{\sigma^2_{Slope} + \sigma^2_{Tracking} + \sigma^2_{Reflector} + \sigma^2_{Sun}} .$$

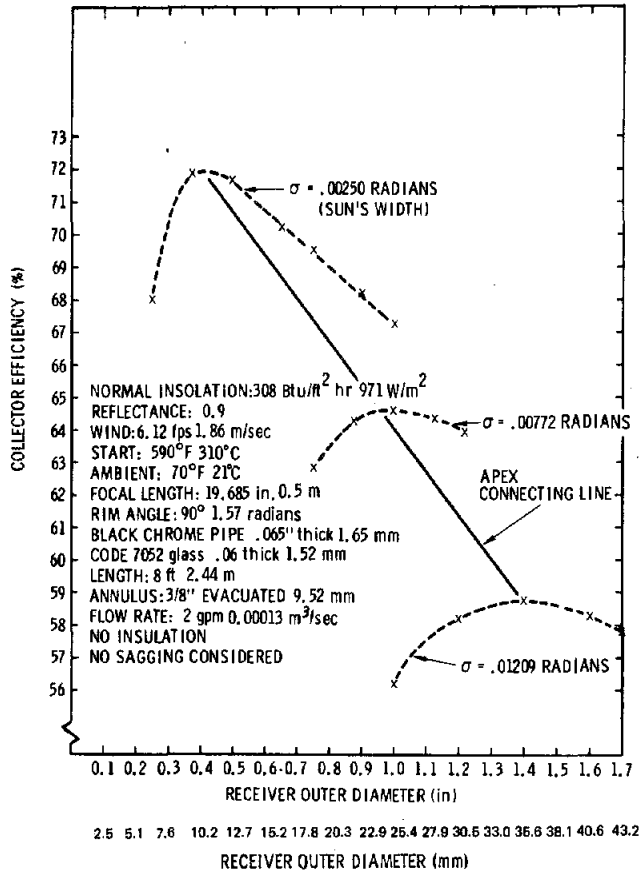


Figure 20. Energy Distribution vs Collector Efficiency

Efforts to characterize the slope errors of parabolic reflector surfaces have been made through the use of the apparatus illustrated in Figure 21. The laser is scanned in the X direction, and the resulting reflection is captured at a particular location on the detector which is located at the focal point such that the angular deviation from the calculated focus can be measured. After each scan, the parabolic mirror is translated to a new Y position. The resulting scans can be portrayed as illustrated in Figure 22 and statistically reduced to a deviation representative of that mirror.

With a  $\pm 2\sigma$  normal distribution (95.46% of the area under a normal curve), recent extremes of measurements on 0.79 radian rim angle parabolas (0.61 m x 1.22 m) can be used as follows:

$$\begin{aligned}
 \text{Beam } \sigma &= \left[ (\text{Sun } \sigma)^2 + (\text{Tracking } \sigma)^2 + (\text{Slope Error } \sigma)^2 + (\text{Reflector } \sigma)^2 \right]^{1/2} \\
 \sigma &= \left[ (2.5 \text{ mrad})^2 + (2.5 \text{ mrad})^2 + (7.9 \text{ mrad})^2 + (2 \text{ mrad})^2 \right]^{1/2} \\
 \sigma &= 8.9 \text{ milliradians.}
 \end{aligned}$$

With this energy distribution, an optimum diameter of 27.4 mm results from entry into Figure 20.

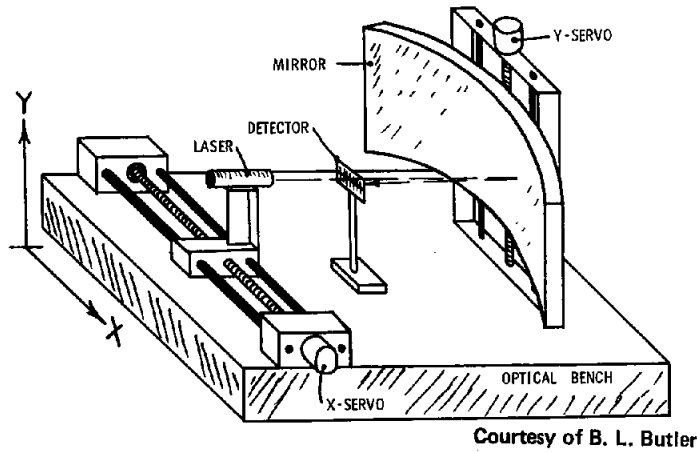


Figure 21. Apparatus for Characterizing Slope Errors of Parabolic Reflector Surfaces

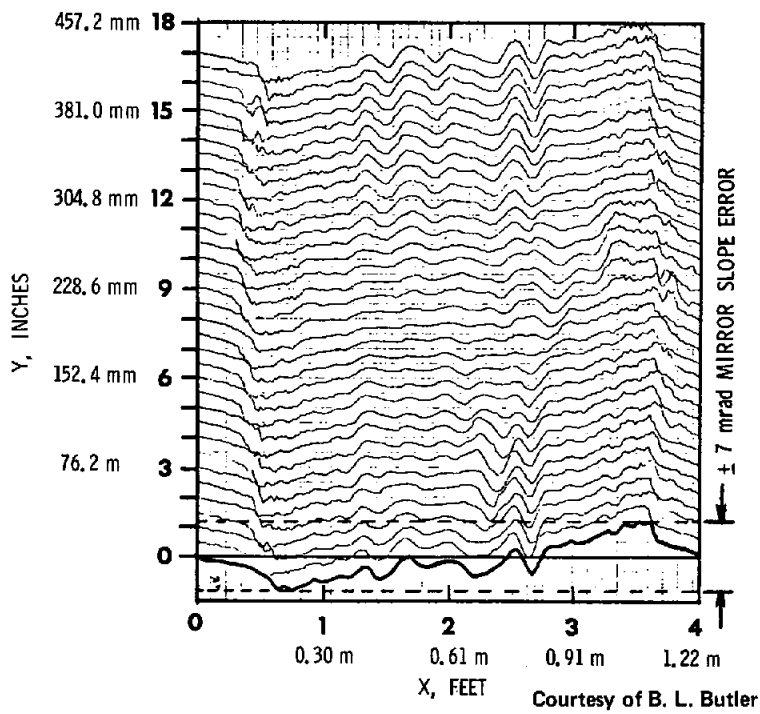


Figure 22. Scans Resulting From Use of Apparatus Shown in Figure 21

With an occluded angle aperture calculated from this receiver, an appropriate specular reflectance can be selected from Figure 16.

The selection of the 1.57 radians (90°) rim angle is now brought back into question since it can be shown that a 2.09 radians (120°) rim angle yields the shortest average distance from the reflector to the focus (See Appendix A) and, ostensibly, the least reflected beam spread. Reference to Figure 23 shows that slight efficiency improvements can be obtained by increasing the rim angle to greater than 1.57 radians with an optimum occurring between a 1.83 radians and a 1.92 radians rim angle. Rim angles less than 1.57 radians; which are not displayed in Figure 23, result in efficiencies lower than that for 1.57 radians. The reason for the slight departure from the 2.09 radians theoretical optimum is due to the thermal considerations and beam spreading at larger angles. The slope and tracking error influences become more pronounced with larger rim angles.

There is a penalty associated with the use of larger rim angles since the arc length changes of reflector required for a given aperture are not in proportion to the increase in efficiency. The sectors of the parabola which have significant slope angles are not contributing as much to solar energy interception. Where the slope of the parabola is 0.79 radian, its aperture for the same reflector arc length is only 70.7% of the parabola aperture near the vertex. An alternative to restricting the parabola slopes would be to trim, figuratively, a 1.57 radians rim angle parabola to 1.40 radians or 1.22 radians while retaining the focus. This removes the most arc length for the least change in aperture. These considerations are reflected in the calculated results given in Tables II and III. Obviously a "trimmed" width must have compensating length to capture the same amount of energy.

It would be desirable to establish a figure-of-merit to use for comparison of these alternatives. All other things being equal, the cost of collector construction is proportional in some manner to the weight or surface area, while the energy collected is proportional to the collector efficiency. Alternative figures-of-merit could be constructed as follows.

$$\text{Figure of Merit} \propto \frac{\text{Construction Cost}}{\text{Energy Collected}} \propto \frac{(\text{Average Receiver Circumference} + \text{Reflector Arc Length})(\text{Collector Length})}{(\text{Collector Efficiency})(\text{Standard Collector Length})}$$

or if it could be determined that reflector arc length had more influence on total cost it could appear as follows:

$$\text{Figure of Merit} \propto \frac{(1/4 \text{ Average Receiver Circumference} + 3/4 \text{ Reflector Arc Length})(\text{Collector Length})}{(\text{Collector Efficiency})(\text{Standard Collector Length})}$$

Table IV lists some results from such calculations using data from Tables II and III. The calculations suggest a "trimmed" collector may be desirable, but they should be viewed with caution since other non-considered factors are not necessarily equal. For "trimmed" rim angles, the smaller diameter receiver tubes may mean greater heat transfer liquid pumping losses, and the longer collector may require more intermediate supports. For larger rim angles, the influence

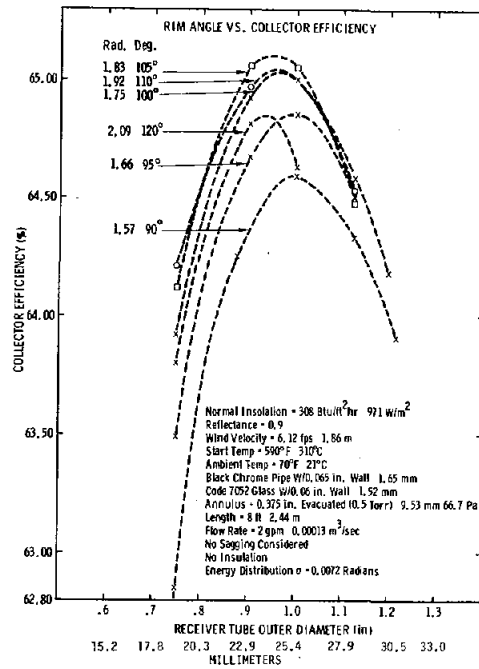


Figure 23. Collector Efficiency vs Receiver Tube Outer Diameter

TABLE II

Phase IVB Collector Sizing Considerations

Rim Angle (rad) (deg)	Approximate Collector Efficiency (%)	Focal Length (mm) (in)	Approx. Optimum Receiver OD (mm) (in)	Arc Length (mm) (in)	Remarks
1.22 70 (Trimmed 90°) 1.57 rad	63.7	500 19.68	22.9 0.9	1.51 59.36	90° Rim Angle Focal Length 1.57 radian 1.4 Metres Aperture
1.40 80 (Trimmed 90°) 1.57 rad	64.3	500 19.68	22.9 0.9	1.85 73.16	90° Rim Angle Focal Length 1.57 radian 1.678 Metres Aperture
0.79 45	55.97	1207 47.52	40.6 1.6	2.06 80.94	2 Metres Aperture
1.05 60	60.6	866 34.10	35.6 1.4	2.11 82.92	2 Metres Aperture
1.22 70	62.4	714 28.11	28.7 1.13	2.15 84.77	2 Metres Aperture
1.40 80	63.8	596 23.46	26.7 1.05	2.21 87.19	2 Metres Aperture
1.57 90	64.6	500 19.68	25.4 1.00	2.30 90.38	2 Metres Aperture
1.66 95	64.9	458 18.04	25.4 1.00	2.35 92.35	2 Metres Aperture
1.75 100	65.0	420 16.52	24.1 0.95	2.40 94.64	2 Metres Aperture
1.83 105	65.1	384 15.10	24.1 0.95	2.47 97.31	2 Metres Aperture
1.92 110	65.0	350 13.78	24.1 0.95	2.55 100.46	2 Metres Aperture
2.09 120	64.8	289 11.37	24.1 0.95	2.76 108.67	2 Metres Aperture

Normal Insulation - 308 Btu/ft<sup>2</sup> hr 971 W/m<sup>2</sup>  
 Reflectance = 0.9  
 Wind Velocity = 6.12 fps 1.86 m/sec  
 Start Temp = 590°F 310°C  
 Ambient Temp = 70°F 21°C  
 Black Chrome Pipe W/0.065 m Wall 1.65 mm  
 Code 7052 Glass W/0.06 in. Wall 1.52 mm  
 Annulus = 0.375 in. Evacuated (0.5 Torr) 9.53 mm 66.7 Pa  
 Length = 8 ft 2.44 m  
 Flow Rate = 2 gpm 0.00013 m<sup>3</sup>/sec  
 No Sagging Considered  
 No Insulation  
 Energy Distribution σ = 0.0072 Radians

of tracking and slope errors becomes more pronounced. Upon brief consideration of these factors, there appears to be no compelling reason at the present time to depart from 1.57 radians (90°) rim angle although indicators point more toward smaller than larger rim angles.

TABLE III  
Collector Efficiency (%) and Arc Length Changes (%)  
Compared to 1.57 Radians (90°) Rim Angle

Rim Angle		Change in Collector Efficiency (%)	Change in Arc Length (%)
Degrees	Radians		
45°	0.79	-13.50	-10.44
60°	1.05	- 6.24	- 8.25
70°	1.22	- 3.39	- 6.21
80°	1.40	- 1.32	- 3.53
95°	1.66	+ 0.40	+ 2.18
100°	1.75	+ 0.63	+ 4.71
105°	1.83	+ 0.73	+ 7.67
110°	1.92	+ 0.62	+11.15
120°	2.09	+ 0.34	+20.24
80° @ 90° focus	1.40 @ 1.57 radian focus	- 0.46	-19.05
70° @ 90° focus	1.22 @ 1.57 radian focus	- 1.38	-34.32

Since the influence of aiming and slope errors has been briefly mentioned, another influencing factor in effective collector design is the accuracy with which the true focal line can be determined. The laser technique mentioned earlier can establish the true focal line for a given parabola and, presumably, such a technique can be used for production acceptance and quality control. However, if separate collectors are arranged in a contiguous manner and "gang" driven, the receiver tube assembly positioning will probably be along an average focal line. The influence of mislocation of a receiver tube assembly is illustrated in Figure 24. For the conditions shown, the receivers can be mislocated only by  $\pm 10\%$  of their diameter without suffering a significant loss in effectiveness. The receiver diameter could be made slightly larger to compensate for mislocation without a significant efficiency penalty as shown in Figure 20.

In summary, a 1.57 radians (90°) rim angle appears reasonable, and the receiver tube diameter can be sized based upon the techniques resulting in the data shown in Figure 20.

TABLE IV

Figure of Merit vs Collector Rim Angle

Rim Angle (rad)	(deg)	Aperture, (m)	Figure of Merit*	Figure of Merit**
1.22	90 (Trimmed to 70) 1.22 rad	1.4	1.419	1.095
1.57	90 (Trimmed to 80) 1.40 rad	1.678	1.431	1.036
0.79	45	2	1.560	1.114
1.05	60	2	1.461	1.050
1.22	70	2	1.434	1.038
1.40	80	2	1.442	1.044
1.57	90	2	1.466	1.066
1.66	95	2	1.491	1.085
1.75	100	2	1.522	1.109
1.83	105	2	1.557	1.137
1.92	110	2	1.612	1.176
2.09	120	2	1.739	1.273

\*Based On: (Average Receiver Circumference + Reflector Arc Length)/(Collector Efficiency)  
(Standard Collector Length)

\*\*Based On: (1/4 Average Receiver Circumference + 3/4 Reflector Arc Length)  
(Collector Efficiency)(Standard Collector Length)

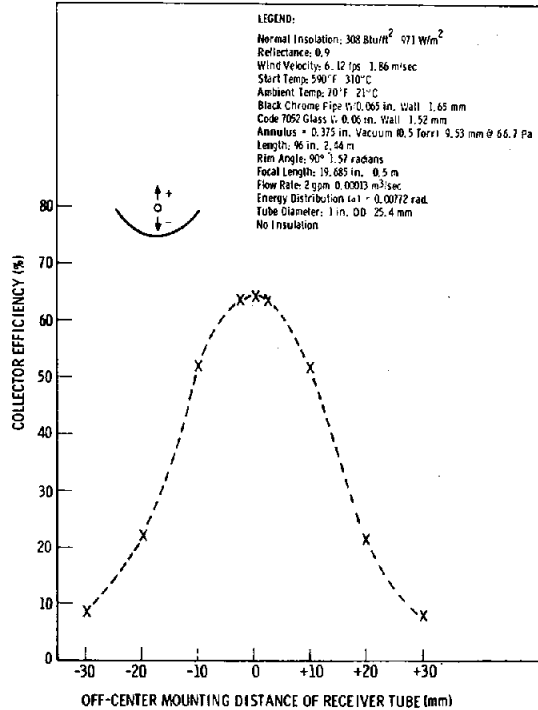


Figure 24. Influence of Off-Center Receiver Tube Mounting

## Collector Sizing

The discussions on receiver sizing have been, to a large extent, based upon the fact of optical congruence. The collector aperture could have been 1 metre or 10 metre wide, and the same conclusions would hold. Once the energy delivery requirements for a collector field are established, other factors must be considered. For a given energy delivery requirement at a specified temperature, the flow rate is established. Heat transfer into the working fluid at a given flow rate is a function of diameter and is not linearly proportional (congruent). To a limit, the energy transfer into the working fluid is enhanced by a smaller receiver diameter. Since this is the situation, the collector aperture can be adjusted to achieve the proper receiver diameter to optimize the collection efficiency. It must be kept in mind that energy delivered is energy collected less energy required to drive the fluid through the collector system. If the pumping losses are kept to some limit, say 1% of the collected energy, and the flow is maintained in the turbulent regime to maintain effective heat transfer, it is possible to establish some collector sizing limits. One such attempt is portrayed on Figure 25. A 2 metre aperture has a higher collector efficiency than a 2.74 metre aperture collector although both collectors have a 1.57 radians rim angle. The 25.4 mm receiver OD associated with a 2 metre aperture is a practical minimum size because of friction losses at the 1% level. As previously suggested, the number or length of collectors must be increased to capture the same quantity of solar energy. More narrow apertures mean smaller supports and frames and smaller structures due to smaller bending moments in wind-loading. Whether those cost reductions compensate for greater numbers or length of collectors remains to be seen. However, if costs are the same, the 2 metre aperture is potentially more effective.

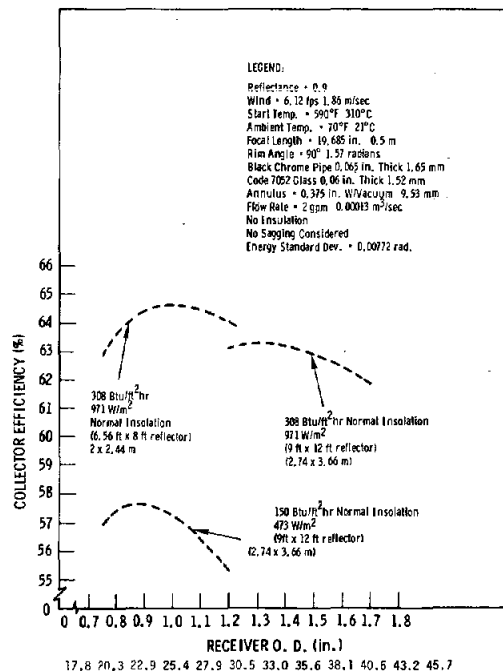


Figure 25. Energy Input Influence on Receiver Sizing

## Influence of Asymmetric Heating

With 1.57 radians rim angle line-focus reflectors, a much greater amount of energy is deposited upon one half of a receiver tube than upon the other half. If the heat transfer liquid and receiver material cannot effectively transfer this energy into the lower energy-deposition areas of the receiver, significant asymmetric heating of the fluid and receiver distortion can occur. For organic heat transfer liquids, allowable film temperature limits can be exceeded which will result in lower heat transfer, viscosity increases, and greater pumping losses. If the liquid boils, the collector system must be designed to withstand the pressures without venting and loss of energy and fluids. The heat transfer ability of a liquid-gas system would not normally be as good as a liquid system due to mass flow considerations. With respect to the foregoing, water is an excellent heat transfer liquid but requires nearly  $11 \times 10^6$  Pa (1600 psi) overpressure at 315°C to prevent boiling. Any storage system for high temperature water has significant safety hazards.

Several possible techniques for better distribution of the energy have been considered. Copper receiver tubes would circumferentially transfer the energy better than steel tubes but are more expensive, more ductile, and require more supports to prevent sagging. Increasing the thickness of the steel tubes would increase the weight of the tube at a greater rate than the moment of inertia is increased and more supports would also be required. The use of internal rods to force annular flow is a technique to better transfer the energy into the liquid by decreasing the hydraulic radius and thereby increasing the film coefficient of heat transfer. Other mixing techniques that require lower pumping work are being investigated. As an indication of the distortion caused by asymmetric temperatures in steel receiver tube 1.6 mm thick, a diametral temperature difference  $\Delta T$  of 56°C can cause an additional 25.4 mm sag over a 3.66 metre span.

Calculations for the organic liquid Therminol 66 (Figure 26) indicate that a  $\Delta T$  of this magnitude can occur. Obvious solutions to prevent the  $\Delta T$  are to use internal rods and to increase the flow rates. These effects are shown in Figure 27. The internal rod delays larger  $\Delta T$ 's until much lower volumetric flow rates are reached. In both cases shown in Figure 27, increasing flow rate decreases the  $\Delta T$  in the liquid. Flow rate control is an important parameter in the use of organic liquids.

## Other Design Considerations

If collectors are oriented on an east-west axis, it is prudent to arrange them contiguously to minimize the energy losses at morning and evening due to high non-normal incidence angles causing end losses. An 18.3 metre length of receiver tubes when heated from ambient to 315°C can expand nearly 76 mm in length. Flexible end joints and linear slides must accommodate this expansion. One design which can be used is illustrated in Figure 28. The pins which fix the receiver tube position also accommodate the expansion by allowing sliding. The pin-hole clearances also allow some end flange rotation due to the receiver  $\Delta T$ . The expansion bellows accommodate the linear expansion differences between the glass and the steel receiver tube.

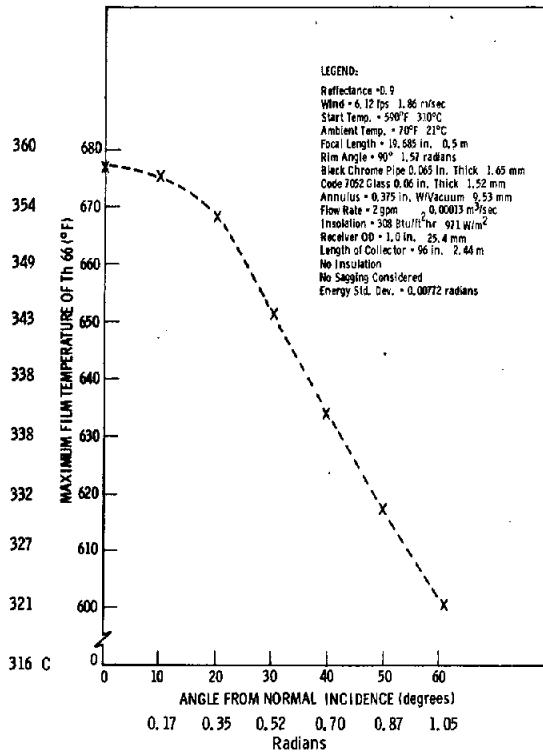


Figure 26. Predicted Maximum Therminol 66<sup>Ⓢ</sup> Film Temperatures

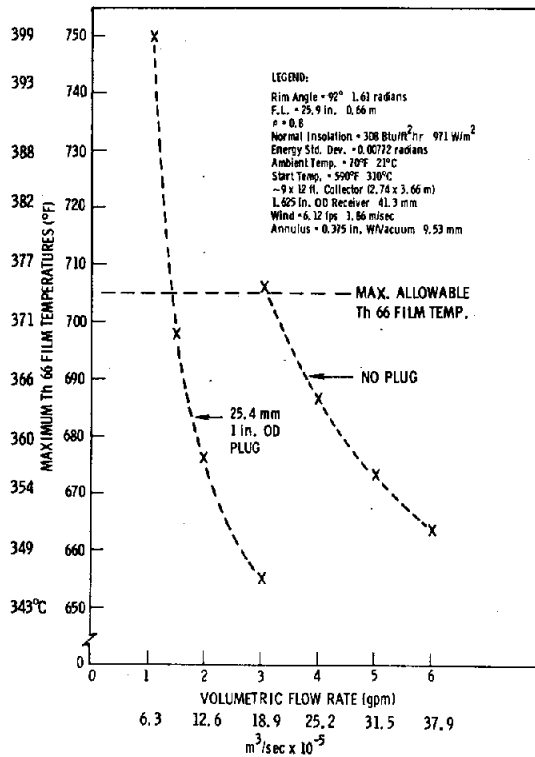


Figure 27. Influence of Plug on Predicted Maximum Therminol 66<sup>Ⓢ</sup> Film Temperatures (Phase IVA Northwest Quadrant)

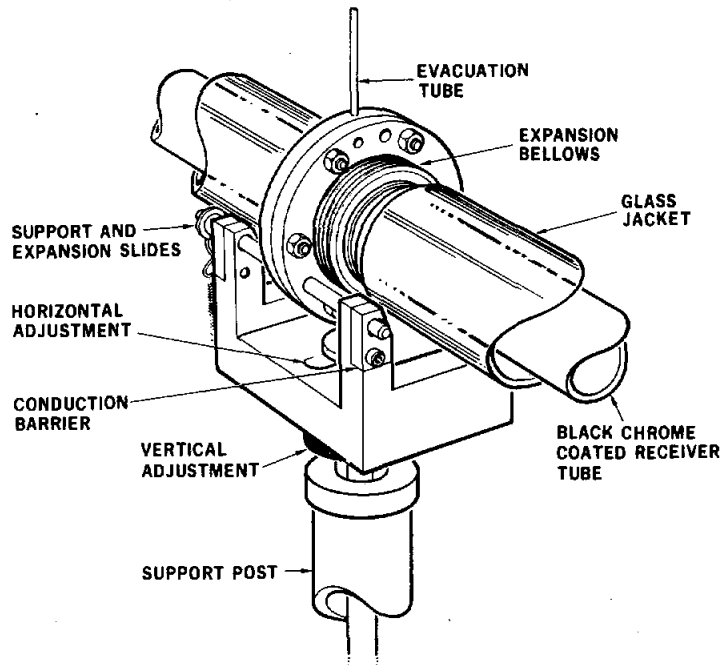


Figure 28. Receiver Tube and Support Assembly

The glass should reach temperatures of less than 110°C although the receiver reaches 315°C. The glass-to-metal seal is formed by expansion-matched borosilicate glass and Kovar. Operation with liquids at 315°C requires durable leak-proof seals. Hollow metal "O" rings are adequate for this design.

The thickness of the receiver tube has been briefly mentioned. The span of the receiver between supports represents a trade-off between deflection and circumferential energy transfer. The thicker the tube material, the greater the sag and the better the energy transfer, and vice versa. The internal rod for obtaining high film coefficients of heat transfer is hollow such that it will "float" in the liquid and not sag against the internal diameter of the receiver tube and exaggerate the receiver sag from the focal line.

Another receiver tube assembly design which appears to be capable of satisfying all requirements is illustrated in Figure 29. In this design, commercial tube fittings and silicone "O" rings replace the flanges, welded joints, expansion bellows, and glass-to-metal seals. Calculations prior to testing and temperatures obtained during testing indicate "survival" of the seal for long periods. In addition, broken glass tubes are easily replaced so repair is inexpensive.

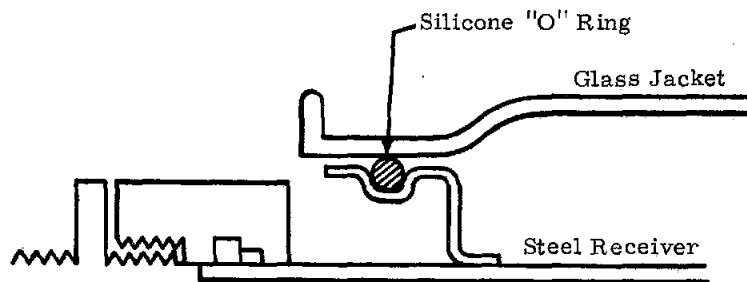


Figure 29. Alternate Receiver Tube Assembly Design

#### Miscellaneous Considerations

The orientation of collectors (N-S axis versus E-W axis) also is involved with trade-offs. The east-west oriented collector arrangement will typically collect less energy than the north-south, but it is more economical in land utilization because of shadowing considerations, lower in construction and pipeline costs, and has less pumping and thermal losses from one collector bank to the next because they can be closer without shadowing. Another consideration is that the east-west collector sunset position is almost exactly the position for sunrise. The north-south must be driven from the evening to the morning position. East-West orientations lend themselves to uniflow receiver designs. An option for counterflow receivers appears to be more appropriate for north-south orientations. At that, the proposed use of counterflow receivers should require detailed thermal analysis because of the asymmetry of energy deposition for parabolic-cylindrical collectors.

East-West linear-focusing collectors with off-axis receivers may offer some promise of construction cost reductions in exchange for less energy collection due to solar aperture and cosine effects. Certainly off-axis receivers can have lower thermal losses due to the insulation which can be used. The selection of the orientation and collector design is a function of the importance of these considerations, the latitude, and the expected amount of sunshine at the site.

APPENDIX A  
 CALCULATIONS OF RIM ANGLE FOR MINIMUM  
 AVERAGE DISTANCE FROM FOCUS TO PARABOLA

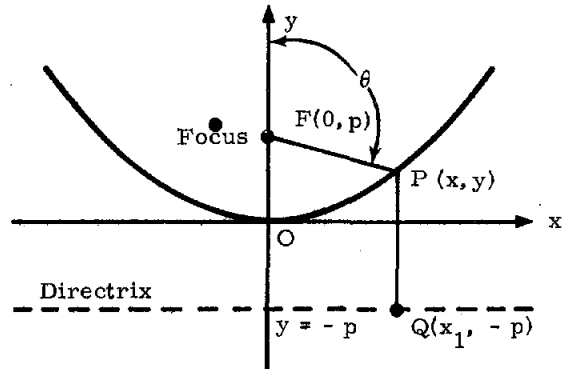
General Formula for Parabola:  $y = \frac{x^2}{4p}$

$$\overline{FP} = r = \left[ x^2 + (p - y)^2 \right]^{1/2}$$

$$r = \left[ x^2 + \left( p - \frac{x^2}{4p} \right)^2 \right]^{1/2}$$

$$r = \left[ \frac{x^2}{2} + p^2 + \frac{x^4}{16p^2} \right]^{1/2}$$

$$r = p + \frac{x^2}{4p}$$



Average distance from focus to parabola:

$$\bar{r} = \frac{\int_0^{X_{\max}} \left( p + \frac{x^2}{4p} \right) dx}{\int_0^{X_{\max}} dx}$$

$$\bar{r} = \frac{px + \frac{x^3}{12p} \Big|_0^{X_{\max}}}{x \Big|_0^{X_{\max}}} = \frac{pX_{\max} + \frac{X_{\max}^3}{12p}}{X_{\max}}$$

$$\bar{r} = p + \frac{X_{\max}^2}{12p}$$

Minimum average distance for  $x = x_{\max}$ :

$$\bar{r} = p + \frac{x_{\max}^2}{12p}$$

$$\frac{d\bar{r}}{dp} = 1 - \frac{x_{\max}^2}{12p^2}$$

$$0 = 1 - \frac{x_{\max}^2}{12p^2}$$

$$p = \frac{x_{\max}}{2\sqrt{3}}$$

$$@ x_{\max} = 1$$

$$p = 0.288675$$

Distance from focus to parabola expressed in polar coordinates:

$$\overline{OF} = p = \frac{r(1 - \cos \theta)}{2}$$

$$@ \theta = 60^\circ \text{ (i.e., rim angle = } 120^\circ)$$

$$x_{\max} = 1$$

$$r = 1.1547$$

$$\text{and } p = \frac{1.1547(1 - \cos 60^\circ)}{2}$$

$$p = 0.288675$$

•• Minimum average distance occurs at  $120^\circ$  rim angle

## Bibliography

- Eldon C. Boes, Solar Radiation Availability to Various Collector Geometries, A Preliminary Study, SAND76-0009, Sandia Laboratories, Albuquerque, New Mexico, March 1976.
- R. B. Pettit, Total Hemispherical Emittance Measurement Apparatus for Solar Selective Coatings, SAND75-0079, Sandia Laboratories, Albuquerque, New Mexico, June 1975.
- D. M. Mattox, et. al., Selective Solar Photothermal Absorbers, SAND75-0361, Sandia Laboratories, Albuquerque, New Mexico, July 1975.
- E. R. G. Eckert, Robert M. Drake, Jr., Analysis of Heat and Mass Transfer, McGraw-Hill, New York, 1972.
- William H. McAdams, Heat Transmission, 3rd Edition, McGraw-Hill, New York, 1954.
- G. W. Treadwell, Selection of Parabolic Solar Collector Field Arrays, SAND74-0375, Sandia Laboratories, Albuquerque, New Mexico, May 1975.
- M. W. Edenburn, Performance of a Focusing Cylindrical Parabolic Solar Energy Collector: Analysis and Computer Program, SLA-74-0031, Sandia Laboratories, Albuquerque, New Mexico, April 1974.
- G. W. Treadwell, et. al., Test Results from a Parabolic-Cylindrical Solar Collector, SAND75-5333, Sandia Laboratories, Albuquerque, New Mexico, July 1975.
- W. H. McCulloch, G. W. Treadwell, Design Analysis of Asymmetric Solar Receivers, SAND74-0124, Sandia Laboratories, Albuquerque, New Mexico, August 1974.
- M. W. Edenburn, N. R. Grandjean, Energy System Simulation Computer Program-SOLSYS, SAND75-0048, Sandia Laboratories, Albuquerque, New Mexico, June 1975.
- Frank Biggs, EDEP: A Computer Program for Modeling the Parabolic Trough Solar Concentrator, SAND76-0106, Sandia Laboratories, Albuquerque, New Mexico, to be published.
- D. M. Mattox, Coatings and Surface Treatments in Solar Energy Applications, Plating and Surface Finishing, January 1976, pp. 55-59.
- D. M. Mattox, Solar Energy Materials Preparation Techniques, Journal of Vacuum Science Technology, Vol. 12, No. 5, Sept/Oct. 1975, pp. 1023-1031.

DISTRIBUTION:

TID-4500-R64, UC-62 (274)

US ERDA

Division of Solar Energy  
Washington, DC 20545  
Attn: G. Kaplan

US ERDA

Albuquerque Operations Office  
P.O. Box 5400  
Albuquerque, NM 87115  
Attn: D. K. Nowlin

Watt Engineering Ltd  
RR 1, Box 183-1/2  
Cedaredge, CO 81413  
Attn: A. D. Watt

1100 C. D. Boyles  
Attn: J. D. Kennedy, 1110  
G. E. Hansche, 1120

1280 T. B. Lane  
1283 H. C. Hardee  
1284 R. T. Othmer  
1300 D. B. Shuster  
1330 R. C. Maydew  
1400 A. Y. Pope  
2300 L. D. Smith  
2320 K. L. Gillespie  
Attn: L. W. Schulz, 2324

2541 G. E. Gobeli  
3620 R. S. Wilson  
3622 E. R. Frye  
5000 A. Narath  
Attn: J. K. Galt, 5100

5110 F. L. Vook  
5130 G. A. Samara  
5150 J. E. Schirber  
5200 E. H. Beckner  
5231 J. H. Renken  
Attn: F. Biggs

5420 J. V. Walker  
5700 J. H. Scott  
5710 G. E. Brandvold  
5711 R. P. Stromberg  
5712 J. A. Leonard  
5712 G. W. Treadwell (100)  
5735 M. M. Newsom  
5740 V. L. Dugan  
5800 R. S. Claassen  
Attn: R. L. Schwoebel, 5820

5830 M. J. Davis  
Attn: D. M. Mattox, 5834

5840 D. M. Schuster (3)  
Attn: R. C. Heckman, 5842  
F. P. Gerstle, 5844  
E. K. Beauchamp, 5846

8100 L. Gutierrez  
8180 C. S. Selvage  
Attn: A. C. Skinrood, 8184

9300 L. A. Hopkins, Jr.  
9330 A. J. Clark, Jr.  
9336 J. V. Otts  
9340 W. E. Caldes  
Attn: J. L. Mortley, 9344

9400 H. E. Lenander  
9410 R. L. Brin  
Attn: R. K. Petersen, 9412

9515 J. T. Hillman  
8266 E. A. Aas (2)  
3141 C. A. Pepmueller (Actg) (5)  
3151 W. L. Garner (3)  
For ERDA/TIC (Unlimited Release)